Improving the Power System Dynamic Response through a Combined Voltage-Frequency Control of Distributed Energy Resources

Weilin Zhong, *IEEE Student Member*, Georgios Tzounas, *IEEE Member*, Federico Milano, *IEEE Fellow*

Abstract— The paper proposes a control scheme to improve the dynamic response of power systems through the automatic regulators of converter-based Distributed Energy Resources (DERs). In this scheme, both active and reactive power control of DERs are varied to regulate both frequency and voltage, as oppsed to current practice where frequency and voltage controllers are decoupled. To assess the proposed control against the current state-of-art, the paper also defines a metric that captures the combined effect of frequency/voltage response at any given bus of the network. Results indicate that the proposed control strategy leads to a significant improvement in the stability and performance of the overall power system. These results are based on a comprehensive case study carried out by employing a modified version of the IEEE 39-bus benchmark system, where a portion of the synchronous machines is substituted by converter-interfaced DERs. The impact on the proposed control of load models, the R/X ratio of network lines, as well as the level of DER penetration to the grid, are properly evaluated and conclusions are duly drawn.

Index Terms— Power system dynamic response, converter-based Distributed Energy Resources (DERs), frequency and voltage regulation, active and reactive power control.

I. INTRODUCTION

A. Motivation

Environmental and sustainability concerns drive the gradual replacement of fossil fuel-based power plants by non-synchronous Distributed Energy Resources (DERs), including renewable sources and storage systems [1]. As the share of DERs to the energy mix increases, their contribution to the frequency and voltage regulation are considered essential services to maintain the stability and performance of the grid [2]. DERs are typically connected to the grid via power electronic converters, which provide high flexibility in their control design as well as the ability to act faster than the controllers of conventional generators [3], [4]. This paper proposes a general control strategy to improve the overall dynamic response of power systems by efficiently exploiting the active and reactive control capabilities of converter-based DERs.

B. Literature Review

As the penetration of converter-based resources to the grid increases, the total amount of rotational inertia decreases. This leads to high frequency variations which, in case of a severe power imbalance, may trigger a system-level collapse [1]. The capability of DERs to regulate the frequency through the available power reserve is limited because (i) they are typically designed to achieve a (near) maximum power extraction; and (ii) the availability of a certain power reserve is hard to be ensured, since a large portion of DER generation is stochastic, e.g. wind and solar photo-voltaic [5].

Frequency regulation in power systems is traditionally provided through the active power, while the reactive power is employed to regulate the voltage. This is an intuitive choice for conventional large-scale systems, where the active (P) and reactive (Q) power flows are largely decoupled due to the highly inductive nature of transmission lines [6]. On the other hand, DERs are often integrated within distribution networks, where the resistance/inductance (R/X) ratio of feeders is large, thus leading to a strong interaction of P and Q with voltage and frequency, respectively. In this vein, a solution that has been proposed is to artificially impose the P-Q decoupling through the control of power converters, e.g. with the application of a virtual impedance control [7], [8]. Instead, in this paper we effectively exploit the P-Q coupling with a scope to improve the frequency and voltage regulation provided by DERs.

In this vein, the authors in [9] study the ability of converter-based resources to regulate the frequency through voltage control, taking advantage of load sensitivity to voltage variations in microgrids. The concept of voltage-based frequency control has been also recently applied to improve the frequency response of large power systems through static var compensators connected to load buses [10], [11]. In addition, a multi-band power system stabilizer to improve the primary frequency response of synchronous machines is proposed in [12]. In [12], the problem of frequency regulation is translated into the one of damping the so-called system frequency regulation mode, see [13]. A reactive power-based frequency control for solar photo-voltaic is presented in [14], while a voltage-based feedback to mitigate the part of DER active power injection that does not contribute to the frequency regulation thus improving the system dynamic response is proposed in [15]. Finally, the authors in [16] study the effect of combined active and reactive power control to the frequency response of

doubly-fed induction generators.

The references above indicate that voltage and reactive power regulation can contribute to the improvement of the frequency response both in small and large scale systems. On the other hand, recent research results show that active power regulation can also be utilized to improve the voltage response of the system. For example, reference [17] proposes a voltage controller through active power management for hybrid fuel-cell/energy-storage distributed generation systems, while an active power-voltage control scheme for islanded microgrids is presented in [18]. Moreover, the authors in [19] propose a voltage regulation strategy that combines the battery management of electric vehicles and the active power curtailment of photo-voltaic, to address voltage variations in distribution networks.

C. Contributions

The specific contributions of the paper are as follows.

- A control scheme that enhances the dynamic response of power systems through the automatic controllers of converter-based DERs. In the proposed scheme, the regulation of both frequency and voltage is provided through both the active and reactive power control loops of DERs. This is in contrast to current practice, where active and reactive power control loops are partially or fully decoupled.
- A novel scalar metric that captures the combined effect of frequency/voltage response provided at a bus of the power network. This metric is sensitive to the rate of change of the frequency and the voltage and thus captures and is able to evaluate the transient performance of the proposed DER active/reactive control scheme under a variety of disturbance scenarios.

The contributions of the paper are supported by a comprehensive study that evaluates the proposed control in comparison to the classic frequency-active power, voltage-reactive power scheme, and assesses the effects on its performance of the behavior of the loads; of the R/X ratio of the network lines; of the level of DER penetration to the grid; and of the system's granularity.

D. Organization

The remainder of the paper is organized as follows. Section II provides the theoretical framework of the paper starting from the well-known power flow equations, and presents a metric to assess the joint voltage/frequency response at any bus of a power network. Section III introduces the proposed DER control strategy for primary frequency and voltage regulation. The case study is discussed in Section IV, based on a modified version of the IEEE 39-bus system. Finally, conclusions are drawn and future work is outlined in Section V.

II. THEORETICAL BACKGROUND

The complex power injection at the network buses of a power system can be described as:

$$\bar{S}(t) = P(t) + jQ(t) = \bar{v}(t) \circ \left(\bar{Y}\,\bar{v}(t)\right)^*, \quad (1)$$

where $P, Q \in \mathbb{C}^{n \times 1}$ are the column vectors of bus active and reactive power injections, respectively; n is the number of network buses; $\bar{Y} \in \mathbb{C}^{n \times n}$ is the network admittance matrix; $\bar{v} \in \mathbb{C}^{n \times 1}$ is the vector of bus voltages; $\circ$ denotes the element-wise multiplication; and $*$ indicates the conjugate. The h-th elements of P and Q can be written as:

$$P_h = \sum_{k=1}^{n} P_{hk} = \sum_{k=1}^{n} v_h v_k \left(G^{hk} \cos\theta_{hk} + B^{hk} \sin\theta_{hk}\right),$$

$$Q_h = \sum_{k=1}^{n} Q_{hk} = \sum_{k=1}^{n} v_h v_k \left(G^{hk} \sin\theta_{hk} - B^{hk} \cos\theta_{hk}\right),$$

(2)

where the time dependency is omitted for simplicity; P_{hk}, Q_{hk} are the active and reactive power flows, respectively, from bus h to bus k; G^{hk} and B^{hk} are the real and imaginary parts of the (h, k) element of $\bar{Y}$, i.e. $\bar{Y}^{hk} = G^{hk} + jB^{hk}$; v_k is the voltage magnitude at bus k, $k = 1, 2, \ldots, n$; and $\theta_{hk} = \theta_h - \theta_k$, where θ_h and θ_k are the voltage phase angles at buses h and k, respectively. Differentiation of (2) gives:

$$dP_h = \sum_{k=1}^{n} \frac{\partial P_h}{\partial \theta_{hk}} d\theta_{hk} + \sum_{k=1}^{n} \frac{\partial P_h}{\partial v_k} dv_k = dP_{\theta,h} + dP_{v,h},$$

$$dQ_h = \sum_{k=1}^{n} \frac{\partial Q_h}{\partial \theta_{hk}} d\theta_{hk} + \sum_{k=1}^{n} \frac{\partial Q_h}{\partial v_k} dv_k = dQ_{\theta,h} + dQ_{v,h},$$

(3)

where $dP_{\theta,h}$, $dQ_{\theta,h}$ are the quota of dP_h and dQ_h that depend on the voltage angles and consequently, the components of the active and reactive power that can be effectively used to regulate the frequency in the system; and $dP_{v,h}$, $dQ_{v,h}$ are the quota of dP_h and dQ_h that depend on the voltage magnitudes and thus the components that can be used to modify the voltage response.

Consider equations (3). Then, the parts of $dP_{\theta,h}$, $dQ_{\theta,h}$ and $dP_{v,h}$, $dQ_{v,h}$ that are due to local variations of the frequency and the voltage at bus h, respectively, are given by the following expressions [20]:

$$dP_{\theta,h}^{\text{loc}} = -Q_h d\theta_h, \quad dQ_{\theta,h}^{\text{loc}} = P_h d\theta_h,$$

$$dP_{v,h}^{\text{loc}} = \frac{P_h}{v_h} dv_h, \quad dQ_{v,h}^{\text{loc}} = \frac{Q_h}{v_h} dv_h.$$

(4)

Then rewriting equations (4) using time derivatives, one has:

$$\frac{dP_{\theta,h}^{\text{loc}}}{dt} = -Q_h \theta_h', \qquad \frac{dQ_{\theta,h}^{\text{loc}}}{dt} = P_h \theta_h', \qquad (5)$$

$$\frac{dP_{v,h}^{\text{loc}}}{dt} = P_h u_h', \qquad \frac{dQ_{v,h}^{\text{loc}}}{dt} = Q_h u_h', \qquad (6)$$

where

$$\theta_h' = \frac{d\theta_h}{dt}, \qquad u_h' = \frac{1}{v_h}\frac{dv_h}{dt}. \qquad (7)$$

The first term, namely θ_h', is the deviation of the bus frequency with respect to the synchronous frequency; whereas u_h' represents the transient rate of change of the voltage normalized with respect to the bus voltage magnitude. The latter quantity has the same unit as a frequency and is thus comparable with the frequency deviation θ_h'.

In the remainder of this paper, we are interested in assessing the combined active/reactive injection effect on the

voltage/frequency response provided at bus h. With this aim we utilize the quantity:

$$\mu'_h = \sqrt{(\theta'_h)^2 + (u'_h)^2}\,. \tag{8}$$

In particular, we are interested in assessing the cumulative effect of μ'_h for a given time interval $[t_0, t]$. This interval is determined based on the time scale of the primary response of generators, which typically lasts from few seconds to few tens of seconds.

Finally, the following quantity is proposed as a metric to assess the joint frequency/voltage response at a given bus h of a power network:

$$\mu_h = \int_{t_0}^{t} \mu'_h \, dt\,. \tag{9}$$

The metric in (9) possesses the property that the two components corresponding to the frequency and voltage are considered with the same weights, while having the same units, thus being summable and directly comparable. In this paper, the metric is used in the case study of Section IV to compare the effectiveness of different DER active/reactive control configurations. With this regard, note that smaller values of μ_h are in general obtained for smaller frequency and voltage variations, which in turn, indicate a better dynamic response at bus h.

III. PROPOSED CONTROL SCHEME

This section describes the structure of the proposed DER control scheme. Since the focus is on the utilization of the active/reactive control loops and on which control signal is dedicated to which control objective, we have chosen to keep each control loop simple yet practical, by employing standard filters and controllers widely used in industrial applications.

Considering a simplified DER model, the block diagram of the control scheme is depicted in Fig. 1. The control scheme consists of an inner current control loop and two outer loops for frequency and voltage regulation, respectively. The current control loop regulates the d and q axis components of the current (i_{d}, i_{q}) in the dq reference frame. These components are limited between their minimum and maximum values through an anti-windup limiter. The frequency control loop receives the frequency error ϵ_ω and applies a droop control and a washout filter acting in parallel. On the other hand, the voltage control loop adjusts the bus voltage error ϵ_v by means of a Proportional-Integral (PI) controller and a washout filter also connected in parallel. The outputs of the frequency and voltage controllers are then added to the DER's active and reactive power references. It is worth observing that we have adopted simple conventional controllers on purpose, as these are the most commonly implemented in practice and to to allow easily reproducing the results presented in the case study. As a matter of fact, the main objective of this work is to show how combining the effect of different control channels impact on the performance of the overall system.

The proposed DER control scheme includes four channels that can be combined to formulate different active and reactive
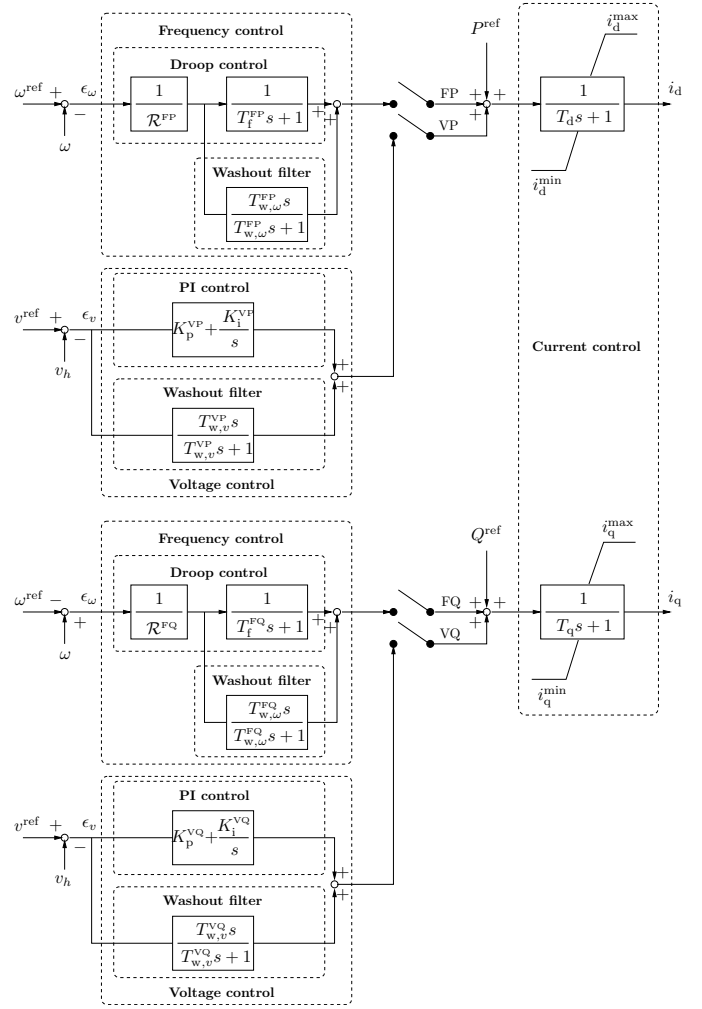

Fig. 1: Proposed DER control scheme.

power control modes. A summary of the available control modes for the active power of the DER is as follows:

- **FP**: The active power is employed to regulate the frequency. The FP mode is the standard way to regulate the frequency in conventional power systems.
- **VP**: The active power is employed to regulate the voltage. In this mode, a voltage control channel acts by modifying the DER active power reference.
- **FVP**: The active power reference is modified to control both the frequency and the voltage. In this case, both FP and VP in Fig. 1 are switched on.

Similarly, the available modes for the control of the DER reactive power can be summarized as follows:

- **VQ**: The reactive power is utilized to regulate the voltage. This is the classic approach, i.e. voltage regulation is conventionally realized by means of the VQ mode.
- **FQ**: The reactive power reference of the DER is modified to provide frequency regulation.
- **FVQ**: Both VQ and FQ are switched on in a combined control of the reactive power.

In this work we study the effectiveness of frequency and voltage regulation provision through both the active and reac-

tive power of DERs, which leads to the combined scheme FVP+FVQ. In the case study of Section IV, the dynamic performance of this configuration is compared to other configurations, including the conventional approach to frequency-voltage control, i.e. FP+VQ.

IV. CASE STUDY

This section presents simulation results based on the IEEE 39-bus benchmark system [21]. The system comprises 10 synchronous machines (Gen 1-10), totaling 6354.1 MW and 1357.1 MVAr of active and reactive power generation. Synchronous machines are represented by 4-th order (two-axis) models and are equipped with automatic voltage regulators, turbine governors, and power system stabilizers. In this paper, synchronous generators are also assumed to participate to secondary frequency regulation through an Automatic Generation Control (AGC) scheme. The AGC is modeled as an integrator (with gain $k_{\text{AGC}} = 0.2$), the output of which is used to update the active power set-points of the machines every 5 s.

TABLE I: Parameters of DER controls.

Controller	Parameters
Current	$T_{\text{d}} = 0.04$ s, $T_{\text{q}} = 0.04$ s
Frequency	$\mathcal{R}^{\text{FP}} = \mathcal{R}^{\text{FQ}} = 0.075$,
	$T_{\text{f}}^{\text{FP}} = T_{\text{f}}^{\text{FQ}} = 0.12$ s, $T_{\text{w},\omega}^{\text{FP}} = T_{\text{w},\omega}^{\text{FQ}} = 0.05$ s
Voltage	$K_{\text{p}}^{\text{VP}} = 1.5$, $K_{\text{p}}^{\text{VQ}} = 5$,
	$K_{\text{i}}^{\text{VP}} = K_{\text{i}}^{\text{VQ}} = 10$, $T_{\text{w},v}^{\text{VP}} = T_{\text{w},v}^{\text{VQ}} = 0.1$ s

Loads are modeled using the ZIP model, the active and reactive power consumption of which, $P_{L,h}$, $Q_{L,h}$, are quadratic expressions of the bus voltage, as follows [22]:

$$
\begin{aligned}
P_{L,h} &= P_{z0}\left(\frac{v_h}{v_0}\right)^2 + P_{i0}\frac{v_h}{v_0} + P_{P0}\,, \\
Q_{L,h} &= Q_{z0}\left(\frac{v_h}{v_0}\right)^2 + Q_{i0}\frac{v_h}{v_0} + Q_{Q0}\,,
\end{aligned}
\tag{10}
$$

where v_0 is the nominal voltage at the load bus; v_h is the measured load bus voltage; P_{z0}/Q_{z0}, P_{i0}/Q_{i0}, P_{p0}/Q_{p0} are the corresponding quota of constant impedance, constant current and constant power consumption, respectively. The ZIP loads in this section consist of 20% constant power (e.g., milling machines), 10% constant current (e.g., electric vehicle chargers), and 70% constant impedance (e.g., heating systems) consumption [23].

For the purpose of this case study, the system is modified to include a 30% penetration of non-synchronous generation. To this aim, the synchronous machines Gen 5, 6 and 8 connected to buses 34, 35 and 37, are substituted by converter-based DERs. Considering the practical capacity of a single DER, the DERs connected to each bus here are not single generation sources but are modelled as a combination of several DERs. The single-line diagram of the modified IEEE 39-bus system is shown in Fig. 2. DERs and their controls are modeled as described in Section III.

The parameters of the frequency, voltage, and inner current controllers of the DERs are given in Table I. The first

estimation of the control parameters of each filter has been obtained by setting the time constants of the corresponding differential equations based on the requirements for the time scale of their action, which leads most of the parameters to lie in a certain range. Then the final values of the parameters have been determined through a trial-and-error procedure. It is also relevant to note that the controllers employed in the paper provide an acceptable response for a wide range of operating conditions. For example, for the droop constants of the primary frequency control, good results are obtained in the range $\mathcal{R} \in [10^{-2}, 10^{-1}]$.

To guarantee a fair comparison, different control modes in the paper are compared keeping constant control parameter settings. Note that, when preparing the case study, we have also tried different approaches, for example we tuned each control mode separately with an aim to achieve the best dynamic response. However, since, as discussed above, the controllers perform well for a relative large range of their parameters, their set up does not modify the main conclusions that are drawn in this section.

All simulation results are obtained using the Python-based power system analysis software tool Dome [24].
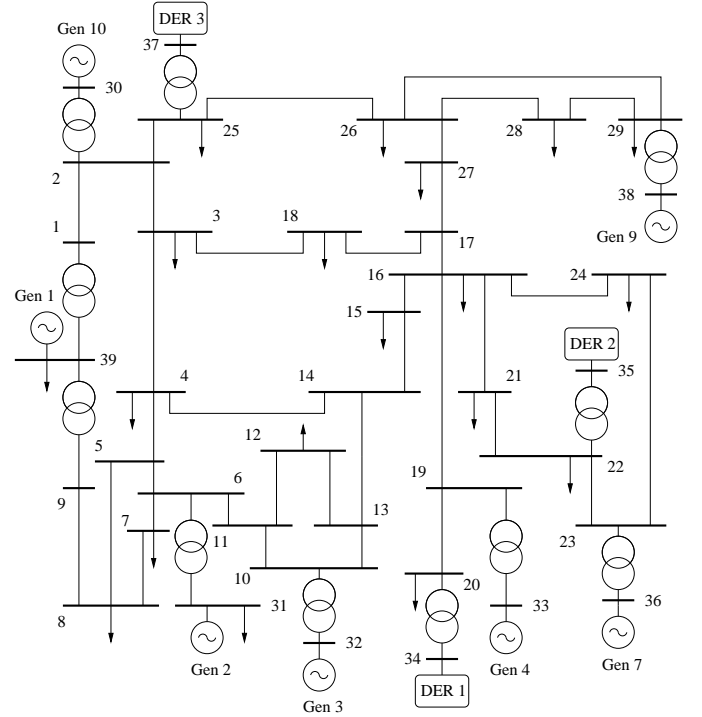

Fig. 2: Single-line diagram of the modified IEEE 39-bus system.

A. Evaluation of FQ and VP Control Modes

In this section, we consider the FQ and VP controls, which are the components that differentiate the proposed FVP+FVQ control strategy from the classical approach, where frequency and voltage regulation are provided only by means of FP and VQ, respectively (see mode definitions in Section III).

We first examine the FQ mode, i.e. the ability of DERs 1-3 to improve the dynamic response of the system by controlling

the frequency through the reactive power. To this aim, the system is simulated for both positive/negative signs of the input control error assuming the tripping of Gen 10 at $t = 1$ s. Results are shown in Fig. 3 where, for the sake of comparison, we have included the response of the system when DERs (i) do not provide any control and (ii) act based on the classic FP control. Figure 3 indicates that the FQ control improves the Center-of-Inertia (CoI) frequency response of the system if utilized with input error $\epsilon_\omega = \omega - \omega^{\mathrm{ref}}$. The main reason for FQ's effectiveness in this case is that the DERs respond to the under-frequency by reducing their reactive power injection and thus the voltage levels at the network. Due to the voltage dependency of loads, see (10), the power demand level decreases, thus reducing the imbalance and helping the recovery of the frequency. Note, finally, that the improvement provided by the FQ mode is lower than the one of the classic FP. This result is as expected. Yet, as it will be seen in Section IV-E, the benefits of using FQ are more apparent when applied at the distribution network level.

(a) CoI frequency.   (b) Voltage at bus 30.

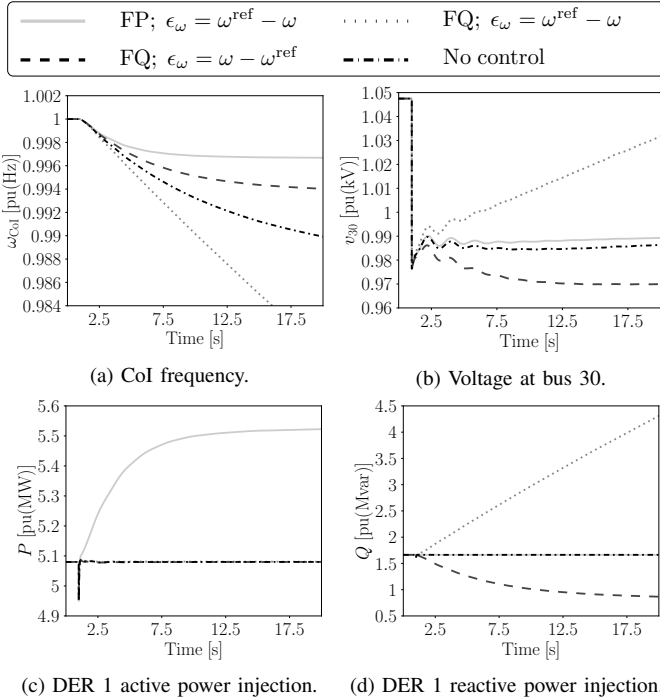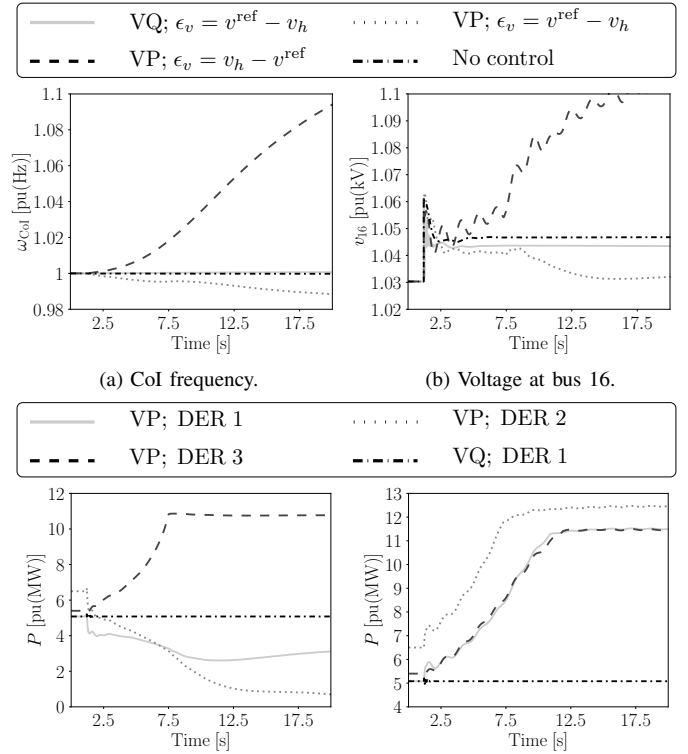(c) DER 1 active power injection.   (d) DER 1 reactive power injection.

Fig. 3: Transient response following the loss of Gen 10.

We show the effect of regulating the voltage at the DER terminal bus through its active power injection, i.e. the VP mode. A simulation is carried out considering the outage of line 15-16 and results are shown in Fig. 4. The VP mode improves the transient behavior of the voltage when the control input error is $\epsilon_v = v^{\mathrm{ref}} - v_h$. However, this mode also introduces large deviations in the power sharing among the DERs connected to the system and thus, using it individually is not suggested. The VP can still contribute to improve the overall system dynamic response if utilized with a relatively small gain and as an auxiliary control that coordinates with other modes. This point is further discussed in the remainder of this case study.

The following remark on the signs of the control input errors

(a) CoI frequency.   (b) Voltage at bus 16.

(c) DERs active power injection. (d) DERs active power injection. VP: Modes VP and VQ ($\epsilon_v = v^{\mathrm{ref}} - v_h$). $\epsilon_v = v_h - v^{\mathrm{ref}}$; VQ: $\epsilon_v = v^{\mathrm{ref}} - v_h$.

Fig. 4: Transient response following the outage of line 15-16.

ϵ_ω, ϵ_v is relevant. For the frequency response of the system to improve, ϵ_ω in FQ has to be the opposite from the one utilized in FP. In terms of the theoretical derivations of Section II, the need for opposite actions when regulating the frequency through the active and reactive power, respectively, can be observed in the structure of (5). On the other hand, to improve the voltage regulation, ϵ_v needs to be implemented with the same sign for both VP and VQ modes. This is consistent with the derivations of Section II, and in particular with (6), which suggests that regulating the voltage variations requires actions in the same direction for both active and reactive power. Hence, $\epsilon_\omega = \omega - \omega^{\mathrm{ref}}$ and $\epsilon_v = v^{\mathrm{ref}} - v_h$ are chosen for FQ and VP in the remainder of the case study.

B. Performance of FVP+FVQ Control

In this subsection, we study the performance of the proposed FVP+FVQ control scheme. This scheme is compared to the classic FP+VQ control, as well as to FP+FQ, VP+VQ, and FP+FVQ. A simulation is carried out considering the disconnection of the load at bus 3 ($P_3 = 3.22$ pu, $Q_3 = 0.024$ pu). The transient behavior of the system following the disturbance is presented in Fig. 5 where, the response of the system with all DER controls disconnected as well as that of the original IEEE 39-bus system serve as references for comparison.

The following remarks are relevant.

- Compared to the original system, a 30% penetration of DERs worsens the overall dynamic behavior of the system, when these resources provide no restorative control actions. This result is as expected.

TABLE II: Frequency/voltage deviations for different contingencies, control modes and load models.

Load model	ZIP						Constant Impedance					
Control	Classic FP+VQ		FP+FQ		FVP+FVQ		Classic FP+VQ		FP+FQ		FVP+FVQ	
$\Delta\omega$ (%)	max	at 20 s	max	at 20 s	max	at 20 s	max	at 20 s	max	at 20 s	max	at 20 s
Load 3 out.	0.5814	0.5946	0.4593	0.4593	**0.2934**	**0.2817**	0.5518	0.5516	0.4082	0.4075	**0.2717**	**0.2637**
Load 20 out.	1.1452	1.1318	0.9476	0.9456	**0.5533**	**0.5202**	1.1378	1.1355	0.8986	0.8985	**0.5501**	**0.5246**
Gen 4 out.	−1.1478	−1.1404	−0.7056	−0.7050	**−0.5141**	**−0.4727**	−1.1029	−1.1028	−0.6199	−0.6158	**−0.4946**	−0.4644
Gen 7 out.	−1.0663	−1.0495	−0.7422	−0.7348	**−0.5393**	**−0.4826**	−1.0408	−1.0325	−0.6711	−0.6685	**−0.5331**	−0.4852
Line 8-9 out.	0.0231	0.0229	0.0180	0.0180	**0.0121**	**0.0118**	0.0804	0.0804	0.0657	0.0655	**0.0537**	**0.0526**
Line 21-22 out.	0.1610	0.1598	0.1544	0.1544	**0.1390**	**0.1354**	0.1994	0.1993	0.1840	0.1837	**0.1612**	**0.1564**
Fault at bus 4	**0.3066**	**−0.0201**	0.3970	−0.0217	0.3505	−0.0238	**0.3543**	0.0294	0.4585	**0.0133**	0.4245	−0.0294
Fault at bus 8	**0.2527**	**0.0042**	0.3182	0.0049	0.2989	0.0059	**0.2865**	0.0276	0.3590	0.0211	0.3257	**0.0150**
Δv (%)	max	at 10 s	max	at 10 s	max	at 10 s	max	at 10 s	max	at 10 s	max	at 10 s
Load 3 out.	1.2867	0.7845	1.7309	1.5417	**1.2533**	**0.6042**	1.2126	0.8275	1.5831	1.4612	**1.1632**	0.6719
Load 20 out.	2.6464	1.5891	6.7898	6.7588	**2.6464**	**1.4299**	2.5097	1.5937	6.4399	6.4291	**2.5097**	1.4550
Gen 4 out.	−7.4634	−3.5033	−10.319	−10.264	**−7.4634**	**−3.2346**	−6.0130	−3.3522	−8.7384	−8.7016	**−6.0130**	−3.1234
Gen 7 out.	−4.8425	−2.9453	−8.0907	−8.0907	**−4.8425**	**−2.8840**	−3.6201	−2.7031	−6.9113	−6.9113	**−3.6201**	−2.6622
Line 8-9 out.	−2.8946	−1.9047	−2.8946	−1.9217	**−2.8946**	−1.9044	**2.3011**	1.7715	2.3376	1.7594	2.3220	**1.7590**
Line 21-22 out.	−6.2882	−4.2634	−6.6219	**−4.1781**	−6.2882	−4.2203	−5.5680	−4.0392	−6.1302	**−3.9151**	−5.5680	−4.0117
Fault at bus 4	−100	−2.1525	−100	**−2.1329**	−100	−2.1749	−100	−2.0802	−100	**−2.0603**	−100	−2.1052
Fault at bus 8	−100	−1.3188	−100	**−1.3138**	−100	−1.3244	−100	−1.2711	−100	**−1.2645**	−100	−1.2762

- The FP+FQ control shows a better frequency response than the classic FP+VQ, yet, it leads to a poor voltage behavior (see Fig. 5b).
- Although the VP+VQ scheme shows a very good voltage response, it leads to a poor frequency response.
- Combining the FP+FQ and VP+VQ modes in a single scheme leads to the proposed FVP+FVQ which provides the best frequency and voltage dynamic response among the schemes compared.

To validate the tuning of the parameters of the controllers and build the trust of the adequateness of this tuning for the stability of the overall system, we have assessed the transient behavior of the system for a wide range of operating conditions and disturbance scenarios. With this aim, we have tested the proposed control under a variety of disturbances, including generator tripping, line outages, short circuits, and load disconnections. Moreover, we have considered the impact of varying the voltage dependency of loads by considering a constant impedance load model. A summary of the results obtained is presented in Table II, where $\Delta\omega$ refers to the relative variation of the frequency of the CoI and Δv refers to the relative variation of a bus voltage magnitude that is local to the disturbance. For each scenario, the table provides the maximum relative variations, as well as the variations few seconds for primary frequency and voltage responses after the disturbance, i.e. at $t = 20$ s of the simulation for the frequency and at $t = 10$ s for the voltage. The smallest frequency/voltage variations obtained for each scenario are marked in bold.

Simulation results suggest that, overall, the proposed FVP+FVQ control leads to an improvement of both primary frequency and voltage regulation of the system. This improvement is significant in case of an outage of synchronous generation, a load switching, or a line trip, while for short circuits, FVP+FVQ performs as the conventional FP+VQ. Finally, note that in contrast to commonly proposed solutions, the performance enhancement provided by FVP+FVQ comes in an inexpensive way, i.e. without the need to install any extra equipment, e.g. storage devices.

TABLE III: Metric μ_{34} (DER 1) for different contingencies, control modes and load models.

Load model	ZIP			Constant Impedance		
Control	FP+VQ	FP+FQ	FVP+FVQ	FP+VQ	FP+FQ	FVP+FVQ
μ_{34}	at 15 s	at 15 s	at 15 s	at 15 s	at 15 s	at 15 s
Load 3 out.	1	0.7891	**0.5467**	1	0.7543	**0.5528**
Load 20 out.	1	0.8283	**0.5327**	1	0.8029	**0.5384**
Gen 4 out.	1	0.6278	**0.4953**	1	0.5816	**0.5187**
Gen 7 out.	1	0.7171	**0.5511**	1	0.6857	**0.5665**
Line 8-9 out.	1	0.8671	**0.7708**	1	0.8192	**0.7315**
Line 21-22 out.	1	0.9544	**0.9101**	1	0.9155	**0.8602**
Fault at bus 4	**1**	1.5189	1.1792	**1**	3.4706	1.5001
Fault at bus 8	**1**	1.5611	1.2027	**1**	1.9155	1.0742

C. Performance of the Proposed Metric μ_h

We study the accuracy of metric μ_h, presented in Proposition 2, to assess the joint voltage/frequency response of DERs. In particular, Table III shows the value of the metric at bus 34, where DER 1 is connected, at $t = 15$ s and for the same disturbances considered in Table II. The value of μ_{34} for each scenario is calculated using the local voltage and its time derivative (v_{34}, dv_{34}/dt) and the variation of the frequency of the CoI ($\Delta\omega_{\mathrm{CoI}}$). Moreover, the results for all control modes are normalized so that the metric for FP+VQ at $t = 15$ s equals to 1. Comparison between Table III

(a) CoI frequency.

(b) Voltage at bus 23.

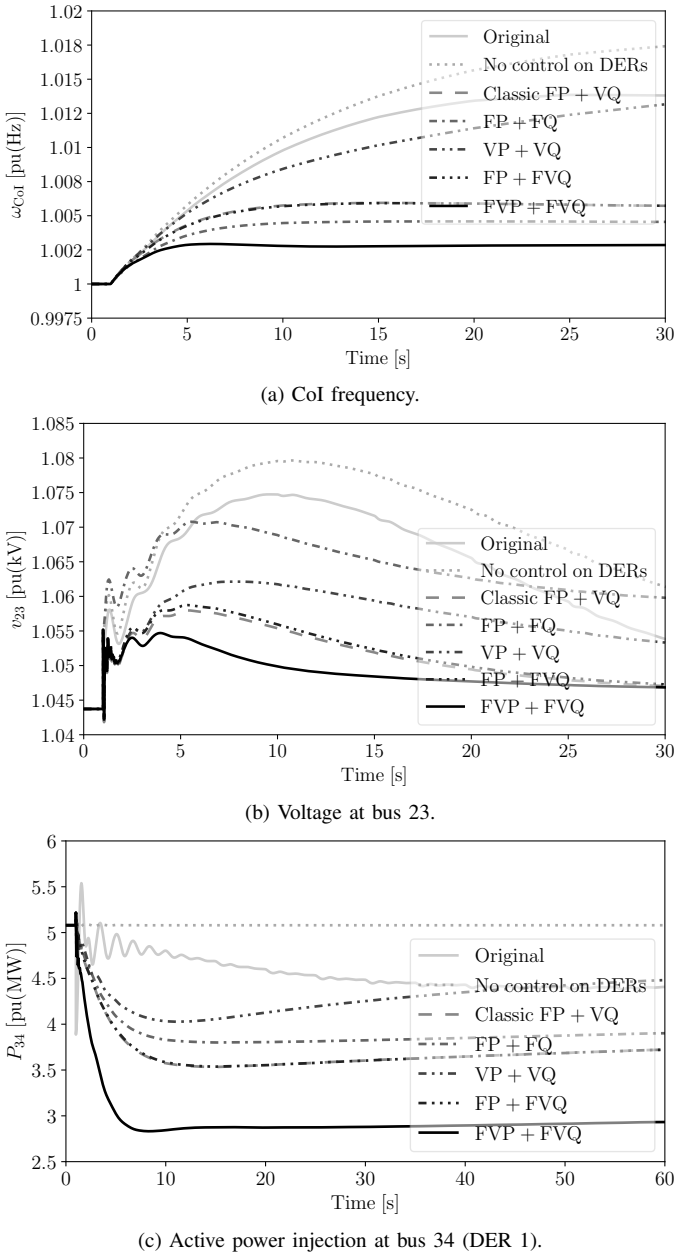(c) Active power injection at bus 34 (DER 1).

Fig. 5: Transient response after disconnection of load at bus 3.

and Table II indicates that the proposed metric can capture the combined voltage/frequency response with good accuracy. With this regard, recall from Section II that smaller values of μ_h imply a better overall dynamic response. It is also worth noting that in the occurrence of a fault at bus 4 and for constant impedance loads, the FP+FQ control shows the worst dynamic response from the metric point of view, although its $\Delta\omega$ and Δv (Table II) are not the worst. In fact, the voltage response for FP+PQ control in this scenario is worse than the other controllers at the first 4 s of the simulation, which is not shown in Table II and it is not observable unless we check the full time-domain response of both the frequency and the voltage. μ_h captures these effects and hence, provides an accurate and convenient way to evaluate the joint frequency and voltage response of DERs. μ_h is utilized as a tool to assess

the performance of DER control modes in the remainder of this case study.

D. Application to Aggregated Power Generation

This scenario assumes that the converter-based resources connected to buses 34, 35, 37 consist of several smaller DERs, the power generation and control modes of which are coordinated through a power aggregation mechanism. This mechanism can be implemented in practice as a Virtual Power Plant (VPP) [25], [26]. For the purpose of this study, we consider that a varying percentage of the DERs that compose the VPP utilize the proposed FVP+FVQ scheme, and the rest act based on the classic FP+VQ control.

Figure 6 shows the results for two disturbances, (a) outage of the line 21-22, and (b) disconnection of the load connected to bus 20 ($P_{20} = 6.28$ pu, $Q_{20} = 1.03$ pu). The results are compared by means of the joint frequency/voltage response metric at bus 34 (μ_{34}), where DER 1 is connected. The metric is calculated as discussed in Section IV-C. As expected, the proposed FVP+FVQ mode has the best performance for both disturbances, which confirms the results shown in Table II. Interestingly, the classic FP+VQ mode combined with 20%-40% FVP+FVQ control worsens the transient response for disturbance (a). We conclude that, depending on practical requirements, the VPP operator can design its assets to apply and/or switch between different control modes.
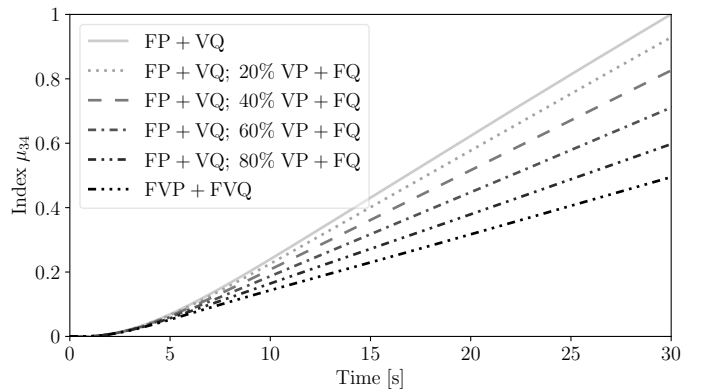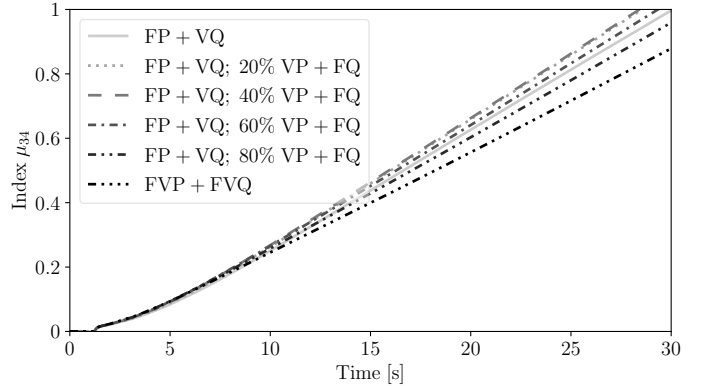

(a) Transient response following the outage of line 21-22.

(b) Transient response following the load disconnection at bus 20.

Fig. 6: μ_{34} (DER 1) for FVP+FVQ applied to a portion of VPP assets.

E. Impact of R/X Line Ratio

In this section, we are concerned with the performance of the proposed control when applied to DERs integrated within distribution networks. To study the distribution network effect, the R/X ratios of the feeders that connect the DERs to the rest of the system are altered so that $R/X \approx 1$. The evolution of μ_{34} for different control modes is presented in Fig. 7, where we have considered the loss of Gen 10 at $t = 1$ s. Moreover, the results are normalized so that for FP+VQ μ_{34} equals to 1 at $t = 30$ s when $R/X \ll 1$. As it can be seen, when $R \approx X$, all DER control modes have a better performance. It is interesting to observe that for $R \approx X$, VP+VQ has the most significant improvement among the examined modes. The same effect can also be observed under different disturbance scenarios in this test system. Finally, the proposed FVP+FVQ control shows the best overall dynamic response among the modes compared.
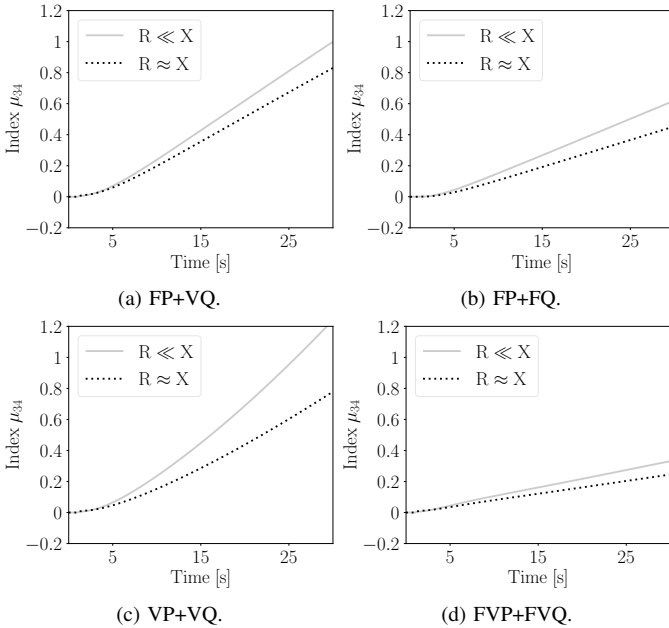

(a) FP+VQ.

(b) FP+FQ.

(c) VP+VQ.

(d) FVP+FVQ.

Fig. 7: Transient response following the loss of Gen 10.

F. Impact of DER Penetration Level

In this scenario we study the impact of the share of DERs to the total generation mix of the system on the performance of the proposed control scheme. To this aim, and in addition to the DERs at buses 34, 35, 37, DERs are also connected to buses 36 and 38, by replacing the local synchronous machines. As a consequence, the penetration of DERs to the modified IEEE 39 bus system increases to 50%. A time-domain simulation of the system is carried out by applying the loss of Gen 10 at $t = 1$ s and results are presented in Fig. 8. As it can be seen, increasing the DER penetration from 30% to 50%, although it leads to a worse voltage response, it does not deteriorate the frequency regulation of the system, which interestingly, slightly improves. Compared to the classic FP+VQ, the FP+FQ outperforms in terms of frequency, but leads to a poor voltage response. As expected, the dual effect holds when the VP+VQ scheme is applied. Most importantly,

the FVP+FVQ control leads to the best dynamic behavior among the examined control modes.
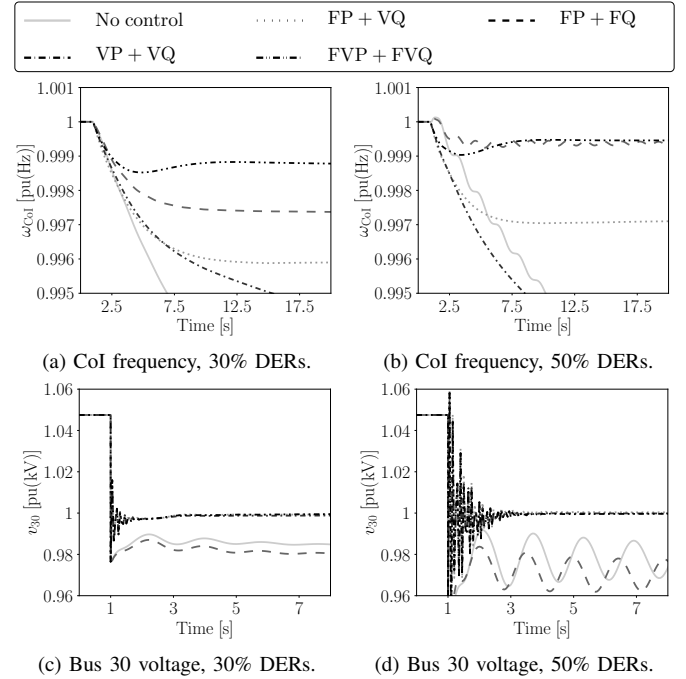

(a) CoI frequency, 30% DERs.

(b) CoI frequency, 50% DERs.

(c) Bus 30 voltage, 30% DERs.

(d) Bus 30 voltage, 50% DERs.

Fig. 8: Transient response following the loss of Gen 10.

G. Impact of System Granularity

In this section we put the emphasis on the effect of the system's granularity and further evaluate the proposed control when employed for resources connected to the distribution level. To this aim, a more detailed modeling of the distribution network and loads is considered. In particular, each of the synchronous generators at buses 32-38 and loads at neighbor buses is substituted with the 8-bus, 38 kV distribution system shown in Fig. 9 [27] (note that, for illustration, in Fig. 9, only one distribution network is shown). As a byproduct, the instantaneous power generation by DERs is increased to 70%. The behavior of loads in this example is represented using the dynamic load model proposed in [28]. Moreover, to account for the proximity of loads, for potential imbalances, as well as for possible harmonics of the power converters, noise has been added on the voltage angle at every bus of the distribution network. Noise is modeled as an Ornstein-Uhlenbeck's process with Gaussian distribution [29].

We carry out a time-domain simulation considering the disconnection of the load at bus 3 at $t = 1$ s. A comparison of the FP+VQ and FVP+FVQ modes is presented in Fig. 10, which indicates that FVP+FVQ leads to an overall better dynamic behavior. Note that the proposed control is in general expected to be more effective and thus lead to larger improvement of the system's response, the higher is the coupling between the active and reactive power flows, i.e. at lower voltage levels and distribution network applications. This is confirmed by Fig. 10, when compared to results discussed in previous sections of this case study, for example with Fig. 5.
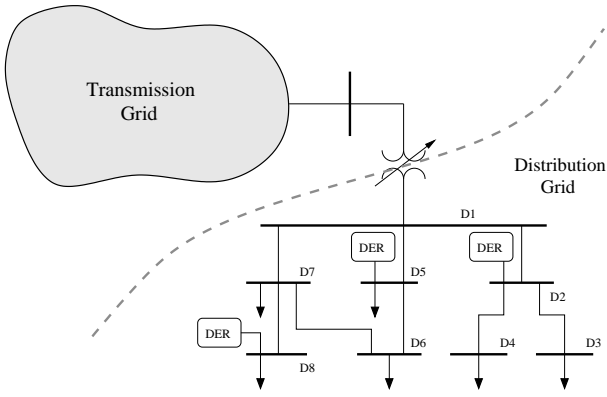
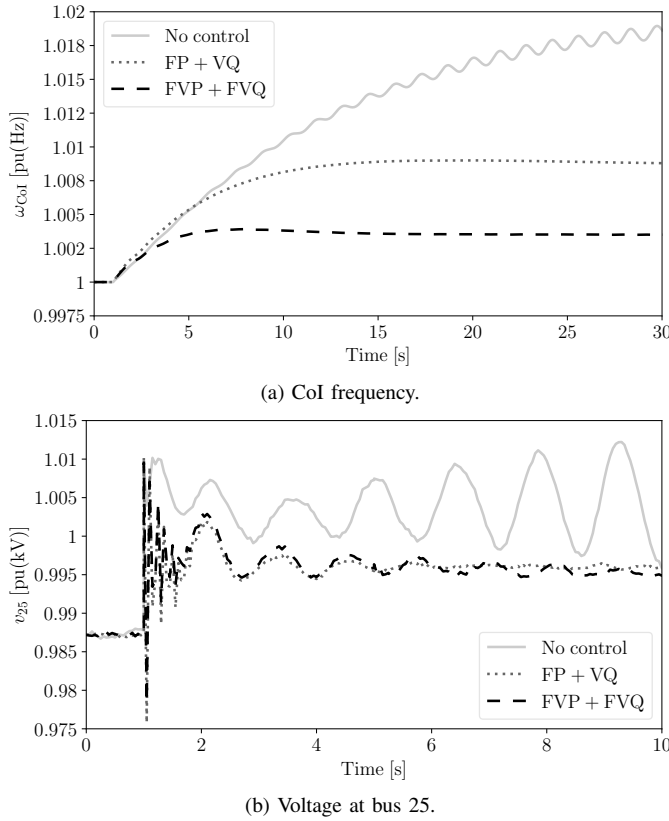Fig. 9: Topology of distribution network model used in Section IV-G.

(a) CoI frequency.

(b) Voltage at bus 25.

Fig. 10: Transient response after disconnection of load at bus 3.

V. CONCLUSIONS

This paper presents a control scheme to improve power system stability through the active and reactive control channels of power electronic converter-based DERs. This scheme is a combined controller in which both active and reactive power injections are modified to compensate both for frequency and voltage variations.

The controller is evaluated in terms of local voltage variations and system CoI frequency dynamic response, as well as in terms of a properly defined joint voltage/frequency response metric. In particular, the proposed metric complements and completes the information provided by the conventional frequency and voltage deviation metrics. Time-domain simulations are carried out considering the effects of load voltage sensitivity, resistance of network lines, and level of DER penetration, and results indicate that, overall, the proposed scheme outperforms other possible active/reactive power control modes and provides a significant improvement to the dynamic response of the system.

Future work will focus on evaluating the proposed control scheme using hardware-in-the-loop tests, on the effect of different network topology and load models, as well as on the impact of switching between different control modes in transient conditions.

REFERENCES

[1] F. Milano, F. Dörfler, G. Hug, D. J. Hill, and G. Verbič, "Foundations and challenges of low-inertia systems," in *Power Systems Computation Conference (PSCC)*. Dublin, Ireland, 2018, pp. 1–25.

[2] N. Hatziargyriou, T. Van Cutsem, J. Milanović, P. Pourbeik, C. Vournas, O. Vlachokyriakou, P. Kotsampopoulos, R. Ramos, J. Boemer, P. Aristidou *et al.*, "Contribution to bulk system control and stability by distributed energy resources connected at distribution network," IEEE, Tech. Rep., 2017.

[3] M. F. M. Arani and E. F. El-Saadany, "Implementing virtual inertia in DFIG-based wind power generation," *IEEE Transactions on Power Systems*, vol. 28, no. 2, pp. 1373–1384, 2012.

[4] D. Ochoa and S. Martinez, "Fast-frequency response provided by DFIG-wind turbines and its impact on the grid," *IEEE Transactions on Power Systems*, vol. 32, no. 5, pp. 4002–4011, 2016.

[5] J. M. Mauricio, A. Marano, A. Gómez-Expósito, and J. L. Martínez Ramos, "Frequency regulation contribution through variable-speed wind energy conversion systems," *IEEE Transactions on Power Systems*, vol. 24, no. 1, pp. 173–180, 2009.

[6] P. Kundur, *Power System Stability and Control*. New York: McGraw-Hill, 1994.

[7] J. M. Guerrero, Luis Garcia de Vicuna, J. Matas, M. Castilla, and J. Miret, "Output impedance design of parallel-connected UPS inverters with wireless load-sharing control," *IEEE Transactions on Industrial Electronics*, vol. 52, no. 4, pp. 1126–1135, 2005.

[8] Y. W. Li and C. Kao, "An accurate power control strategy for power-electronics-interfaced distributed generation units operating in a low-voltage multibus microgrid," *IEEE Transactions on Power Electronics*, vol. 24, no. 12, pp. 2977–2988, 2009.

[9] M. Farrokhabadi, C. A. Cañizares, and K. Bhattacharya, "Frequency control in isolated/islanded microgrids through voltage regulation," *IEEE Transactions on Smart Grid*, vol. 8, no. 3, pp. 1185–1194, 2017.

[10] Y. Wan, M. A. A. Murad, M. Liu, and F. Milano, "Voltage frequency control using SVC devices coupled with voltage dependent loads," *IEEE Transactions on Power Systems*, vol. 34, no. 2, pp. 1589–1597, 2018.

[11] M. A. A. Murad, G. Tzounas, M. Liu, and F. Milano, "Frequency control through voltage regulation of power system using SVC devices," in *Proceedings of the IEEE PES General Meeting*, 2019, pp. 1–5.

[12] A. Moeini and I. Kamwa, "Analytical concepts for reactive power based primary frequency control in power systems," *IEEE Transactions on Power Systems*, vol. 31, no. 6, pp. 4217–4230, 2016.

[13] F. Wilches-Bernal, J. H. Chow, and J. J. Sanchez-Gasca, "A fundamental study of applying wind turbines for power system frequency control," *IEEE Transactions on Power Systems*, vol. 31, no. 2, pp. 1496–1505, 2016.

[14] E. Munkhchuluun, L. Meegahapola, and A. Vahidnia, "Reactive power control of PV for improvement of frequency stability of power systems," in *Proceedings of the IEEE PES General Meeting*, 2020, pp. 1–5.

[15] G. Tzounas and F. Milano, "Improving the frequency response of DERs through voltage feedback," in *Proceedings of the IEEE PES General Meeting*, 2021, accepted in Mar. 2021, available at http://faraday1.ucd.ie/.

[16] C. Tu, J. Cao, L. He, and Y. Fang, "Combined active and reactive power control strategy to improve power system frequency stability with DFIGs," *The Journal of Engineering*, vol. 2017, no. 13, pp. 2021–2025, 2017.

[17] A. Hajizadeh, M. A. Golkar, and A. Feliachi, "Voltage control and active power management of hybrid fuel-cell/energy-storage power conversion system under unbalanced voltage sag conditions," *IEEE Transactions on Energy Conversion*, vol. 25, no. 4, pp. 1195–1208, 2010.

[18] Z. Jiang and X. Yu, "Active power-voltage control scheme for islanding operation of inverter-interfaced microgrids," in *Proceedings of the IEEE PES General Meeting*, 2009, pp. 1–7.

[19] M. Zeraati, M. E. H. Golshan, and J. M. Guerrero, "A consensus-based cooperative control of PEV battery and PV active power curtailment for voltage regulation in distribution networks," *IEEE Transactions on Smart Grid*, vol. 10, no. 1, pp. 670–680, 2017.

[20] J. Arrillaga and N. Watson, *Computer Modelling of Electrical Power Systems*. New York: John Wiley & Sons, 2001, ch. 4, pp. 81–128.

[21] Illinois Center for a Smarter Electric Grid (ICSEG), "IEEE 39-Bus System," URL: http://publish.illinois.edu/smartergrid/ieee-39-bus-system/.

[22] F. Milano, *Power System Modelling and Scripting*. London: Springer, 2010.

[23] J. V. Milanovic, K. Yamashita, S. M. Villanueva, S. Ž. Djokic, and L. M. Korunović, "International industry practice on power system load modeling," *IEEE Transactions on Power Systems*, vol. 28, no. 3, pp. 3038–3046, 2012.

[24] F. Milano, "A Python-based software tool for power system analysis," in *Proceedings of the IEEE PES General Meeting*, Jul. 2013, pp. 1–5.

[25] W. Zhong, M. A. A. Murad, M. Liu, and F. Milano, "Impact of virtual power plants on power system short-term transient response," *Electric Power Systems Research*, vol. 189, p. 106609, 2020.

[26] W. Zhong, J. Chen, M. Liu, M. A. A. Murad, and F. Milano, "Coordinated control of virtual power plants to improve power system short-term dynamics," *Energies*, vol. 14, no. 4, p. 1182, 2021.

[27] C. Murphy and A. Keane, "Local and remote estimations using fitted polynomials in distribution systems," *IEEE Transactions on Power Systems*, vol. 32, no. 4, pp. 3185–3194, 2016.

[28] K. Jimma, A. Tomac, K. Vu, and C. Liu, "A study of dynamic load models for voltage collapse analysis," in *Proc. Bulk Power System Voltage Phenomena, Voltage Stability and Security NFS Workshop*, Deep Creek Lake, Maryland, August 1991.

[29] F. Milano and R. Zárate-Miñano, "A systematic method to model power systems as stochastic differential algebraic equations," *IEEE Transactions on Power Systems*, vol. 28, no. 4, pp. 4537–4544, 2013.

Weilin Zhong (S'19) received the BE degree from Hunan University, China in 2016, and MSc in Advanced Control and System Engineering from the University of Manchester, UK, in 2017. Since February 2018, he is a Ph.D. candidate with University College Dublin, Ireland. His current research interests include inertia estimation and frequency control of virtual power plants, stability analysis and control of distributed energy resources and co-simulation for power systems and communication networks.

Georgios Tzounas (M'21) received the M.E. degree in Electrical and Computer Engineering from the National Technical Univ. of Athens, Greece, in 2017, and the Ph.D. degree in Electrical Engineering from Univ. College Dublin, Ireland, in 2021. From Jan. to Apr. 2020, he was a Visiting Researcher at Northeastern Univ., Boston, MA. He is currently a Postdoctoral Researcher at University College Dublin, working with the EU H2020 project EdgeFLEX. His research interests include modelling, stability analysis and control of electric power systems.

Federico Milano (F'16) received from the University of Genoa, Italy, the ME and Ph.D. in Electrical Engineering in 1999 and 2003, respectively. From 2001 to 2002, he was with the Univ. of Waterloo, Canada. From 2003 to 2013, he was with the Univ. of Castilla-La Mancha, Spain. In 2013, he joined the Univ. College Dublin, Ireland, where he is currently Professor of Power Systems Control and Protections and Head of Electrical Engineering. His research interests include power systems modeling, control and stability analysis.